HHS Public Access

Author manuscript

Neuropharmacology. Author manuscript; available in PMC 2022 February 01.

Published in final edited form as:

Neuropharmacology. 2021 February 01; 183: 108398. doi:10.1016/j.neuropharm.2020.108398.

Topographic transcriptomics of the nucleus accumbens shell: Identification and validation of fatty acid binding protein 5 as target for cocaine addiction

Elizabeth J. Crofton, Ph.D.[1,2,*], **Miroslav N. Nenov, Ph.D.**[1,*], **Yafang Zhang, Ph.D.**[1,3,*], **Cynthia M. Tapia**[1,2], **Joseph Donnelly**[1], **Shyny Koshy, Ph.D.**[1], **Fernanda Laezza, M.D., Ph.D.**[1], **Thomas A. Green, Ph.D.**[1]

[1]Dept. of Pharmacology and Toxicology, Center for Addiction Research, Mitchell Center for Neurodegenerative Diseases, University of Texas Medical Branch, Galveston, TX, 77555, USA

[2]Neuroscience Graduate Program University of Texas Medical Branch, Galveston, TX, 77555, USA

[3]Pharmacology and Toxicology Graduate Program University of Texas Medical Branch, Galveston, TX, 77555, USA

Abstract

Substance use disorders for cocaine are major public health concerns with few effective treatment options. Therefore, identification of novel pharmacotherapeutic targets is critical for future therapeutic development. Evolution has ensured that genes are expressed largely only where they are needed. Therefore, examining the gene expression landscape of the nucleus accumbens shell (NAcSh), a brain region important for reward related behaviors, may lead to the identification of novel targets for cocaine use disorder. In this study, we conducted a novel two-step topographic transcriptomic analysis using five seed transcripts with enhanced expression in the NAcSh to identify transcripts with similarly enhanced expression utilizing the correlation feature to search the more than 20,000 *in situ* hybridization experiments of the Allen Mouse Brain Atlas. Transcripts that correlated with at least three seed transcripts were analyzed with Ingenuity Pathway Analysis (IPA). We identified 7-fold more NAcSh-enhanced transcripts than our previous analysis using single voxels in the NAcSh as the seed. Analysis of the resulting transcripts with

Thomas Green, Center for Addiction Research, Mitchell Center for Neurodegenerative Diseases, Department of Pharmacology and Toxicology, The University of Texas Medical Branch, 301 University Dr., T.G. Blocker Medical Research Building, 7.102C, Galveston, TX 77555-1059, tom.green@utmb.edu, Phone: (409) 747-7056.

Elizabeth Crofton, Miroslav Nenov and Yafang Zhang contributed equally. **Elizabeth Crofton:** Conceptualization; data curation; formal analysis; methodology; investigation; visualization; Writing – original draft**. Miroslav Nenov:** Conceptualization; data curation; formal analysis; investigation; visualization; writing – review & editing. **Yafang Zhang:** Conceptualization; data curation; formal analysis; methodology; investigation; visualization; writing – review & editing**. Cynthia Tapia:** Data curation; formal analysis; investigation**. Joseph Donnelly:** Investigation**. Shyny Koshy:** Validation; investigation; data curation**. Fernanda Laezza:** Conceptualization, funding acquisition, project administration, resources, supervision, writing- review & editing. **Thomas Green:** Conceptualization, investigation, visualization, funding acquisition, project administration, resources, supervision, writing – review & editing

*These authors contributed equally

IPA identified many previously identified signaling pathways such as retinoic acid signaling as well as novel pathways. Manipulation of the retinoic acid pathway specifically in the NAcSh of male rats via viral vector-mediated RNA interference targeting fatty acid binding protein 5 (FABP5) decreased cocaine self-administration and modulates excitability of medium spiny neurons in the NAcSh. These results not only validate the prospective strategy of conducting a topographic transcriptomic analysis, but also further validate retinoic acid signaling as a promising pathway for pharmacotherapeutic development against cocaine use disorder.

Keywords

Topographic transcriptomics; retinoic acid; FABP5; drug addiction; nucleus accumbens

1. Introduction

Cocaine use disorder (CUD) is a highly prevalent disorder characterized by compulsive cocaine taking, which currently has no FDA approved pharmacotherapeutic. Identification of novel targets is therefore critical for future development of effective treatments for CUD. We aimed to identify novel therapeutic targets for CUD through genome-wide investigation of the nucleus accumbens shell (NAcSh) and subsequent evaluation of one novel target via cocaine self-administration with complementary electrophysiological analyses.

Evolution influences gene expression and ensures that genes are expressed largely only where they are needed. As a result, transcripts with enhanced expression in a specific region over neighboring regions may be particularly critical for the function of that region. Thus, transcripts with enhanced expression in the NAcSh may be critical for reward-related behaviors and may influence the development of substance use disorders. The nucleus accumbens is an important region in the reward circuitry and the shell, in particular, plays an important role in the responses to cocaine as cocaine induces release of dopamine in the shell and rats will self-administer cocaine directly into the NAcSh (Pontieri et al., 1995; McKinzie et al., 1999). Our work and others have shown that cocaine causes gene expression alterations in the NAcSh and manipulation of genes in the NAcSh can alter cocaine taking and seeking behaviors and the excitability of NAcSh MSNs (Wallace et al., 2008; Larson et al., 2011; Zhang et al., 2014; Zhang et al., 2016b; Crofton et al., 2017; Scala et al., 2018). Indeed, genes that have proven roles in the regulation of reward related behaviors show enhanced expression in the shell compared to other striatal regions, including cocaine and amphetamine regulated transcript (CART), serotonin receptor 2C (HTR2C), and activating transcription factor 3 (ATF3) (Douglass et al., 1995; Douglass and Daoud, 1996; McMahon and Cunningham, 1999; Green et al., 2008).

The term “topological” in this context refers to the Oxford dictionary definition of “relating to the arrangement of the physical features of an area”. *In situ* expression studies are useful to define the extent of physical brain regions especially when there are no clear histological boundaries, such as between the NAcSh and the rest of the striatum. We hypothesized that a prospective discovery-based analysis of the NAcSh would identify transcripts with enhanced NAcSh expression, which may be involved in the regulation of reward-related behaviors and

that a bioinformatic analysis of the resulting transcripts would identify a novel pathway important for the function of the NAcSh. We utilized the Allen Mouse Brain Atlas (ABA) (Ng et al., 2009; Thompson et al., 2014), a freely-available online resource with genome-wide *in situ* hybridization data of the entire mouse brain (mouse.brain-map.org), to probe for genes with specific expression in the NAcSh over nearby regions, particularly the rest of the striatum, and analyzed pathway level relationships of the resulting genes with Ingenuity Pathway Analysis (IPA). After identifying a promising pathway for further investigation, we validated the novel pathway by manipulating the pathway *in vivo* in the NAcSh of male rats and assessing alterations in cocaine self-administration and complementary alterations in synaptic activity and intrinsic excitability of medium spiny neurons (MSNs), the main neuronal population of the NAcSh.

We previously conducted a different topographic transcriptomic analysis of the NAcSh utilizing the Anatomic Gene Expression Atlas (AGEA) function of the ABA using a seed voxel in the NAcSh to search the ABA, which resulted in a list of 176 genes with enhanced expression in the NAcSh (Zhang et al., 2016a). The ABA contains *in situ* hybridization experiments of the more than 20,000 transcripts in the adult mouse brain in 100μm coronal and 200μm sagittal slices. However, the AGEA is constrained only to transcripts that have data in the coronal plane, which only constitutes 4,376 transcripts in total; therefore, the previous analysis was restricted to this considerably smaller number of transcripts. We aimed to expand the topographic analysis of the NAcSh to all of the transcripts in the mouse genome by utilizing the correlation tool (Thompson et al., 2014) of the atlas in a two-step process. Rather than using a specific seed voxel in the NAcSh, the new analysis used five transcripts with enhanced expression in the NAcSh to search for transcripts with similar expression patterns in the striatum. We first manually identified five seed transcripts with enhanced expression in the NAcSh from the previous topographic transcriptomic analysis (Figure 1). In the second step, we used the five seed transcripts and the correlation tool of the ABA to search for transcripts with similar expression patterns to the five seed transcripts. Only transcripts with expression similar to 3 or more seeds were then analyzed with Ingenuity Pathway Analysis. The advantage of this strategy is that the correlation tool pulls from both sagittal and coronal experiments (>20,000 experiments) rather than the comparably limited 4,376 coronal experiments.

The retinoic acid (RA) signaling pathway (termed *RAR Activation* in IPA) was one of the novel statistically significant pathways in the current analysis, which was not found in the previous analysis. Retinoic acid is a metabolite of retinol, or vitamin A, and is critically important for a variety of functions, especially embryonic pattern development, development of the nervous system, as well as maintaining the adult nervous system (Maden, 2007; Duester, 2008). Retinoic acid is found throughout the brain, including the striatum (Kane et al., 2008). Retinoic acid exerts effects by binding to ligand activated nuclear receptors and typically activates transcription of hundreds of downstream targets (Balmer and Blomhoff, 2002; Maden, 2007) which are involved in a variety of functions and several are related to reward signaling, such as dopaminergic receptors and cholinergic receptors (Balmer and Blomhoff, 2002; Niewiadomska-Cimicka et al., 2017). Additionally, there is some previous evidence that retinoic acid signaling is involved in the regulation of neuronal activity (Aoto et al., 2008; Chen et al., 2014), however the role of retinoic acid signaling in the NAc had

not previously been identified or investigated until our recent studies (Zhang et al., 2016a; Zhang et al., 2019).

In this pathway, fatty acid binding protein 5 (FABP5) is the most NAcSh-enhanced transcript and was one of the 64 transcripts identified by both analyses. As an RA binding protein, FABP5 plays an important role in the RA pathway by translocating RA from the cytoplasm to the nucleus to activate peroxisome proliferator-activated receptors (PPARs). In order to validate the genome-wide topographic transcriptomic analysis, we specifically knocked down FABP5 in the NAcSh of adult male rats with RNA interference via a novel adeno-associated viral vector (AAV). We assessed both cocaine self-administration and alterations in electrophysiology following knockdown of FABP5 in the male rat NAcSh.

2. Materials and Methods

2.1 Topographic transcriptomics of the NAcSh

We manually examined the expression patterns of the top 50 transcripts from our previous topographic analysis of transcripts in the coronal plane in the NAcSh (4,376 transcripts) (Zhang et al., 2016a) and identified five transcripts with highly specific expression in the NAcSh with limited expression in neighboring regions (e.g. Islands of Calleja, NAc core, dorsal striatum). The five seed transcripts identified are CARTPT (cocaine and amphetamine regulated transcript prepropeptide, also known as CART), NTN1 (netrin 1), SMUG1 (single-strand-selective monofunctional uracil-DNA glycosylase 1), STARD5 (steroidogenic acute regulatory (StAR) related lipid transfer domain containing 5), and STRA6 (stimulated by retinoic acid 6) (Figure 1). We used these five transcripts as the seeds for a genome-wide correlation analysis of all the transcripts in the Allen Mouse Brain Atlas (ABA, >20,000 transcripts vs. 4,376 in the previous analysis). We searched for each seed gene in the atlas data portal (mouse.brain-map.org), selected the coronal experiment identified from the previous analysis (CARTPT: 72077479, NTN1: 74511838, SMUG1: 73992919, STARD5: 70813909, STRA6: 75041492), and searched with the correlation tool by selecting “Striatum (STR)” in the correlation tool panel and unselecting “basic cell groups and regions”. We did not select “coronal data only” in order to include all the transcripts in the database.

The correlation for each seed gene results in a rank list of all the transcripts in the database based on a Pearson’s correlation coefficient of the expression pattern of the seed transcript in the striatum (Thompson et al., 2014). We exported the top 2,000 transcripts from each seed gene into Excel. Data can be exported from the ABA by selecting “show 100 genes per page”, viewing the data in XML format, saving the data as an XML file, and importing the XML file into Excel. Using Excel, we removed duplicate transcripts (often transcripts are identified in both the coronal and sagittal experiments) as well as transcripts that were identified in only one or two seed transcript correlations. The resultant list of transcripts correlating with at least three seed transcripts was analyzed for pathway level relationships via Ingenuity Pathway Analysis (Qiagen, www.qiagenbioinformatics.com/products/ingenuity-pathway-analysis/), with the Canonical Pathways analysis and Upstream Regulators analysis. IPA determines whether a query list of transcripts are overrepresented in curated gene sets from a “Knowledge Base” of interactions between genes, chemicals, and molecules from peer-reviewed publications. IPA calculates a p-value for the curated

gene sets with Fisher's Exact Test. Canonical Pathways are gene sets organized by a shared cellular pathway while the Upstream Regulators analysis predicts drugs, molecules, or other genes that are upstream of the genes in the query data set. An overview of the topographic transcriptomic methodology is shown in Figure 2A.

2.2 Animals

Male Sprague-Dawley rats were obtained at 225–249g (behavioral testing) or post-natal day 21 (electrophysiological analysis) (Harlan, Houston, TX). Male rats were pair-housed and maintained in an Association for Assessment and Accreditation of Laboratory Animal Care (AALAC) approved colony and procedures were approved by the UTMB Institutional Animal Care and Use Committee and conform to the NIH Guide for the Care and Use of Laboratory Animals. Male rats were used to validate the bioinformatic analysis conducted with male mouse tissue from the Allen Mouse Brain Atlas, however future work is needed to assess sex as a biological variable and the role of RA signaling in the female NAc.

2.3 Manipulation of target pathway, RA signaling, in the rat NAcSh via knockdown of fatty acid binding protein 5 (FABP5)

In order to manipulate RA signaling *in vivo*, we designed and constructed a novel AAV vector using RNA interference to knockdown expression of FABP5 in the NAcSh of adult rats (Zhang et al., 2019). In order to decrease the expression of FABP5 *in vivo*, five shRNA sequences were designed to target the rat FABP5 coding region (Hommel et al., 2003; Zhang et al., 2019). The five constructs were co-transfected into HEK293 cells with a plasmid that overexpresses rat FAPB5 to determine the most efficient hairpin construct. The most efficient hairpin (5'.GGAAGGGAAAGAAAGCACGATAAC.3'; 96% knockdown of mRNA and 28% knockdown of protein, Supplemental Figure 1) was packaged into an AAV2 capsid (UNC Vector Core) that co-expresses eGFP (shFABP5) (Zhang et al., 2019). An advantage of this method is that AAV2 transduces primarily neuronal cells and only reduces expression of FABP5 if the cell expresses FABP5, thus the knockdown is a physiologically relevant decrease in expression compared to a global knockout. The knockdown efficiency found with the shFABP5 vector is within a similar range of other hairpin driven knockdown vectors we and others have produced(Hommel et al., 2003; Benzon et al., 2014; Zhang et al., 2016a; Crofton et al., 2017; Zhang et al., 2019). The control vector expressed a previously validated control hairpin not targeted to any gene (Benzon et al., 2014; Zhang et al., 2016a; Crofton et al., 2017; Zhang et al., 2019). Viral titer was determined by the UNC Vector core via qPCR (control shRNA titer 1.4×10^{12}vg/ml; shFABP5 titer 4.6×10^{12}vg/ml) (Zhang et al., 2019). The shFABP5 vector or control non-targeted hairpin vector (n=10–12 each) was injected bilaterally into the male rat NAcSh with methods described previously (Zhang et al., 2016a; Crofton et al., 2017; Zhang et al., 2019). Representative titer using immunofluorescence staining for GFP is shown in Figure 6A. Control and shFABP5 vectors were injected bilaterally using coordinates AP=1.7, L=2.2, D=−6.7 for behavioral tests or AP=1.5, L=1.8, V=−5.9 for electrophysiological recordings at a 10° lateral angle (1μl/side over 10 min) under ketamine/xylazine anesthesia. Placement of viral vector injections in the NAcSh for the behavioral tests are shown in Figure 6B. The injection needles remained in place for 10 minutes post-injection to allow for spread of the vector throughout the NAcSh. For behavioral testing, three weeks after surgery, rats

underwent a number of depression, anxiety, and motivation behavioral tasks before cocaine self-administration, including locomotor activity, elevated plus maze, sucrose neophobia (1% w/v liquid), sucrose preference (1% sucrose over water), social contact, cold-stress induced defecation, forced swim test, operant sucrose pellet responding at 85% free-feed body weight and again at 100% free-feed body weight. None of these depression, anxiety, or motivational tests produced statistically significant results (Zhang et al., 2019). A schematic of the timeline of behavioral testing is shown in Figure 6C.

2.4 Cocaine self-administration

At 8 weeks post vector injection, male rats were implanted with a Silastic catheter (0.2 mm I.D.) into the jugular vein, exiting the skin via an external port on the rat's back. Catheters were infused with 0.1 mL of flushing solution (heparin 30.0 U/mL, ticarcillin 250,000 U/mL, streptokinase 8,000 IU/mL, dissolved in sterile saline) daily in order to prevent infection and promote catheter patency for the duration of the study. Rats recovered from catheter implantation for one week prior to acquisition of cocaine self-administration. Accurate placements of the viral vectors were verified immunohistochemically after the conclusion of behavioral testing (Figure 6B). All rats were included in analysis.

2.4.1 Acquisition: One week after catheter surgery, all rats were placed in operant chambers (30 × 24 × 21 cm; Med-Associates, St. Albans, VT) and allowed to self-administer 0.2 mg/kg/infusion unit dose of cocaine for 2 hours per session for 5 days; then 0.5 mg/kg/infusion for 3 days both on a fixed ratio (FR1) schedule. Each infusion was delivered intravenously in a volume of 0.1 ml over 5.8 sec. The infusion was signaled by illumination of two cue lights for 20 sec, which signaled a timeout period during which no further infusions could be obtained.

2.4.2 Fixed ratio dose response: Each rat (control shRNA or FABP5 knockdown) was allowed to self-administer 0.5, 0.25, 0.125, 0.06, 0.03, 0.015, 0.0075, 0.00325 mg/kg/infusion cocaine within-session in descending order on an FR1 schedule each day for five consecutive days. Rats self-administered each dose of cocaine for 30 min.

2.4.3 Extinction: Stably responding rats underwent a within-session extinction procedure for 3 days. All rats were allowed to self-administer 0.5mg/kg/infusion unit dose of cocaine under an FR1 schedule for 1 hour followed by cued extinction for 3 hours. During the extinction period, lever presses resulted in cue-light illumination under an FR1 schedule, but the pump did not deliver cocaine infusions.

2.4.4 Reinstatement: All rats received 0.5mg/kg/infusion unit dose of cocaine under an FR1 schedule for 1 hour followed by 3 h of cued extinction. Next, all rats received an IP injection of cocaine of one of five doses (0, 2.5, 5, 10, 20mg/kg) in a random order for each rat across the five sessions, followed by 3 h of reinstatement responding.

2.4.5 Statistical Analysis of Cocaine Self-administration—Two-factor analyses of variance (ANOVAs) and two-factor repeated measures ANOVAs were performed to compare four treatment groups. Significance between only two conditions was analyzed using a

Student's t-test. All t-test data passed the Shapiro-Wilk test of normality. All data are expressed as mean ±SEM. Statistical significance was set at $p<0.05$.

2.5 Electrophysiology Methods

2.5.1 Slice preparation: Coronal slices with the NAcSh were prepared from control and shFABP5 male rats 21–30 days post-injection as previously described (Crofton et al., 2017). Rats were decapitated, brains were dissected and 300μm coronal slices were prepared with a VT1200S vibratome (Leica Microsystems, Wetzlar, Germany) in cold Tris-based artificial cerebral spinal fluid (aCSF) cutting solution, consisting of the following (in mM): 72 Tris HCL, 18 Tris-BASE, 2.5 KCl, 1.2 NaH2PO4, 25 NaHCO3, 20 HEPES, 25 glucose, 5 sodium ascorbate, 3 sodium pyruvate, 10 MgSO4 and 0.5 CaCl2, 20 Sucrose, osmolarity 300–310 and continuously oxygenized and equilibrated to pH 7.4 with a mixture of 95% O_2/5% CO_2 gases. Tris-based aCSF cutting solution used in the present work was adopted with slight modifications from Dr. Jonathan Ting (brainslicemethods.com/recipes) and provided a high survival rate of NAc neurons in our rat brain slice preparations (Crofton et al., 2017; Scala et al., 2018). Slices were transferred to an incubation chamber with standard aCSF consisting of the following (in mM): 124 NaCl, 3.2 KCl, 1 NaH2PO4, 26 NaHCO3, 1 MgCl2, 2 CaCl2, 10 glucose, osmolarity 300–310, oxygenated and equilibrated to pH 7.4 with a mixture of 95% O_2/5% CO_2 at 31°C for 30 minutes and then at room temperature for 1–2 hours before whole cell patch clamp recordings.

2.5.2 Whole cell patch clamp recordings and data analysis: After recovery for 1–2 hours, acute coronal brain slices containing the NAcSh were placed in a submerged recording chamber on the stage of an upright microscope (Axioskop2 FS plus; Zeiss). Slices were continuously perfused at 30–32 °C (TC-344B temperature controller, Warner Instruments, Hamden, CT, USA) with standard aCSF (~2mL/min) and equilibrated for 15–20 minutes prior to recordings. Whole cell patch-clamp recordings were obtained from visually identified MSNs showing green fluorescence (i.e. transduced by control or shFABP5 vectors). Recording pipettes (3–5 MΩ) were fabricated from borosilicate glass (WPI) using a two-step vertical puller PC-10 (Narishige), and filled with an internal solution containing (in mM) 145 K-gluconate, 2 $MgCl_2$, 0.1 EGTA, 2 Na_2ATP, and 10 HEPES (pH 7.2 with KOH; 290 mOsm). Whole cell recordings were performed using Multiclamp 700B amplifier (Molecular Devices, Sunnyvale, CA). Data acquisition and stimulation were performed with a Digidata 1322A Series interface and pClamp 9 software (Molecular Devices). Data were filtered at 2 kHz and digitized at 20 kHz. Spontaneous excitatory glutamatergic synaptic transmission and neuronal excitability were recorded and analyzed as described previously (Nenov et al., 2014; Nenov et al., 2015). Briefly, spontaneous excitatory postsynaptic currents (sEPSCs) in MSNs were recorded in voltage clamp mode at −70 mV holding potential. 20 μM of bicuculline was added to the standard aCSF in order to block GABAergic inhibitory responses. Then the recording configuration was switched to current clamp mode to assess intrinsic firing and passive and active electrical properties. MSNs were held at −70mV with constant current injection and series of 800 ms long current pulses (from −20 to +200 pA, 10 pA increments with 5 second inter-pulse interval) were applied to elicit trains of action potentials (Scala et al., 2018). Input-output relationships were plotted as number of action potentials against given current steps. Only action

potentials with robust overshoot were included in the analysis. Series resistance (Rs) was monitored throughout the recording and was typically <25 MΩ. All cells with Rs > 25 MΩ were excluded from further analysis. All electrophysiology data were analyzed with pCLAMP 10 and GraphPad Prism 6 software and significance was set at $p<0.05$ with Student's *t*-test or two-way ANOVA for repeated measurements followed by posthoc Fisher's LSD test.

3. Results

3.1 Topographic transcriptomics of the NAcSh of male mice reveals Retinoic Acid Signaling Components

Using the Allen Mouse Brain Atlas correlation tool and five seed transcripts, we identified 236 transcripts significantly correlating with all five seed transcripts, 746 transcripts with four or five seeds and 1,426 transcripts that correlated with at least three of the five seed transcripts (CART, NTN1, SMUG1, STARD5, and STRA6; see supplemental data for all). The NAcSh *in situ* hybridization and expression images from the ABA for each of the five seed transcripts is shown in Figure 1. We used IPA to investigate the functional relationships of the resulting NAcSh specific transcripts, including overrepresented canonical pathways and upstream regulators. IPA could not identify 205 of the transcripts and were therefore excluded from the analysis. IPA therefore analyzed the pathway level relationships of 1,217 NAcSh specific transcripts.

There were 130 canonical pathways identified by this two-step method as significantly overrepresented via IPA of the NAcSh specific transcripts including *Axonal Guidance Signaling* (−log (*p*) = 3.31), *GABA Receptor Signaling* (−log (*p*) = 1.47), and $G\alpha_I$ *Signaling* (−log (*p*) = 1.42, Figure 2B; see supplemental data for all). The new transcript seed method thus identified 4-fold more canonical pathways compared to the 28 pathways identified by the previous one-step AGEA seed voxel method (Zhang et al., 2016a). The NAc utilizes GABA signaling and GPCRs as well as genes related to axonal guidance. Thus, although these are not novel canonical pathways, they bolster confidence in this set of transcripts. An upstream regulator that was identified is CREB1 (−log (*p*) = 6.20), Figure 2C), which has previously been shown to be important for the function of the NAc (Pliakas et al., 2001; Barrot et al., 2002; McClung and Nestler, 2003; Dong et al., 2006; Green et al., 2006; Wallace et al., 2009; Green et al., 2010; Larson et al., 2011; Bilbao et al., 2014), adding additional confidence to this new list of NAcSh transcripts.

One canonical pathway significant in the two-step topographic analysis, but not in the previous one-step analysis, is *RAR Activation* or retinoic acid receptor activation (−log (*p*) = 1.4, Figure 2B). A custom pathway with only the core retinoic acid signaling components is shown in Figure 3B, overlaid with NAcSh specific transcripts identified with the two-step analysis (filled/purple symbols, −log (*p*) = 1.86). The core retinoic acid pathway illustrates the various genes involved in the trafficking and signaling of retinoic acid. Retinoic acid (RA) enters the cell or is synthesized from retinol in the cytoplasm. RA can be degraded into retinoic acid metabolites by CYP26B1, or associate with binding partners FABP5 (fatty acid binding protein 5) or CRABP2 (cellular retinoic acid binding protein 2). FABP5 delivers RA to peroxisome proliferator-activated receptor delta (PPARD) and retinoid x receptors (RXR),

where it regulates transcription of genes with PPAR response elements (PPREs) (Schug et al., 2007). In contrast, CRABP2 delivers RA to RXR and retinoic acid receptors (RAR), regulating transcription through retinoic acid receptor response elements (RARE) (Schug et al., 2007). In this manner, retinoic acid regulates the expression of hundreds of downstream targets. As shown in Figure 3B, genes identified with the topographic transcriptomic analysis of the NAcSh are involved in the trafficking of retinol and RA (STRA6 and FABP5) as well as involved in RA transcriptional regulation (RAR and RXR). Additionally, IPA analysis of the topographic transcriptomic data found that 111 of the NAcSh specific transcripts are downstream of retinoic acid (i.e. tretinoin, $-\log(p) = 2.23$, Figure 3A). Therefore, the topographic transcriptomic analysis of the NAcSh clearly points to retinoic acid signaling as a promising pathway for further investigation.

3.2 Comparison of the current two-step topographic transcriptomic analysis with the previous one-step AGEA analysis

Interestingly, Figure 4A shows that the current analysis only identified 64 of the 176 transcripts from the original AGEA analysis (Zhang et al., 2016a). However, the current topographic analysis was able to identify a number of NAcSh-enhanced targets not identified by the AGEA analysis such as Arnt2 (aryl hydrocarbon receptor nuclear translocator 2, Figure 4B; experiment 71358590), Kcnh1 (potassium voltage-gated channel, subfamily H member 1, Figure 4C; experiment 73636099) and Slit2 (slit homolog 2, Figure 4D; experiment 79591683). The Slit2 result is important in light of its binding partner Robo1 is also highly NAcSh-enhanced as determined only by the previous AGEA analysis. Figure 4E depicts a comparison scatterplot of the significant 130 IPA canonical pathways in the current analysis vs. the 28 from the previous AGEA analysis. Note that *RAR Activation* is statistically significant in the current analysis where it was not in the previous.

3.3 Validation of FABP5 knockdown via novel AAV vector

FABP5 was identified by the topographic transcriptomic analysis as a NAcSh specific transcript (Figures 3, 5). The knockdown efficiency of the shFABP5 vector was validated previously in HEK293 cells and showed more than 96% knockdown at the mRNA level in vitro and approximately 28% knockdown at the protein level in HEK293 cells(Supplemental Figure 1) (Zhang et al., 2019). It should be noted that the qPCR primers and shRNA were targeted only to rat mRNA, but the antibody detected both the rat protein and the human protein from HEK cells, thus accounting for apparent differences in knockdown from mRNA vs. protein. Our previous study showed that FABP5 knockdown did not significantly alter anxiety- and depression-like behavior in rats (Zhang et al., 2019). Representative titer is shown in Figure 6A and relative placements of control and shFABP5 in the NAcSh are shown for the behavior animals in Figure 6B.

3.4 Knockdown of FABP5 in the male rat NAcSh decreases cocaine self-administration

Nine weeks after viral vector injection of shFABP5 or control vector, all rats started cocaine self-administration (Figure 6C). For acquisition of cocaine, there were significant main effects of session ($F(4, 80) = 8.031$, $p < 0.001$) and vector ($F(1, 20) = 7.238$, $p = 0.014$) at the low unit dose of cocaine (0.2mg/kg/infusion, Figure 6D). There was also a significant main effect of session ($F(2, 40) = 6.230$, $p = 0.004$), with a trend for decreased maintenance

responding in FABP5 knockdown rats (F (1, 20) = 4.176, $p = 0.054$) at a high unit dose of cocaine (0.5mg/kg/infusion, Figure 6E). As a model of craving, the cocaine within-session extinction paradigm revealed that knocking down FABP5 in the NAcSh produced a trend for decreased drug-seeking behavior (F (1, 21) = 3.083, $p = 0.094$; Figure 6F). Knocking down FABP5 in the NAc shell caused a rightward shift of the ascending limb of the dose response curve with a significant interaction of dose × vector (F (7, 119) = 4.713, $p < 0.001$; Figure 6G), indicating decreased responding to low unit doses of cocaine. Knocking down FABP5 in the NAc shell did not change the responding to cocaine-induced within-session reinstatement (data not shown). Overall, rats with FABP5 knocked down in the NAcSh exhibited decreased cocaine taking that was more pronounced at lower unit doses and possibly decreased cocaine seeking behavior (i.e. a trend).

3.5 Knockdown of FABP5 in the male rat NAcSh has no effect on spontaneous excitatory glutamatergic synaptic transmission but modulates intrinsic excitability of MSNs

To study the potential mechanisms underlying decreased cocaine self-administration upon FABP5 knockdown, whole-cell patch clamp was used to record spontaneous excitatory postsynaptic currents and intrinsic firing of MSNs in the NAcSh. We found that FABP5 knockdown did not affect spontaneous excitatory synaptic transmission in NAcSh MSNs (Figure 7) since no significant changes either in sEPSC frequency or amplitude were observed (Figures 7B and C). However, FABP5 knockdown significantly altered MSN intrinsic firing (Figure 8). We observed a significant interaction between current step and FABP5 knockdown in current-evoked action potentials ($F_{(19, 684)} = 4.467$, $p<0.0001$, two-way repeated measures ANOVA, Figure 8A and B) and a significant effect of current step injection ($F_{(19, 684)} = 62.98$, $p<0.0001$, two-way ANOVA, Figure 8A and B). Posthoc analysis of the input-output curve revealed a reduction in the number of spikes at middle range of injected current steps in MSNs expressing AAV-shFABP5 compared to shControl MSNs. For example, 12.17±2.39 spikes in control versus 6.35±2.39 in shFABP5 group for firing train evoked with 70 pA current step (t=2.433; df=720, $p=0.015$ with posthoc Fisher's LSD test following two-way ANOVA; Figure 8A and B). At the same time, significant elevation in AAV-shFABP5 MSNs firing was observed for action potentials evoked in response to current injection of high intensity or 200 pA (17±2.39 spikes in control versus 22.85±2.39 in shFABP5 group firing train evoked with 200 pA current step; t=2.447; df=720; $p=0.015$ with posthoc Fisher's LSD test following two-way ANOVA; Figure 8A and B). We observed a significant decrease in instantaneous firing frequency in MSNs expressing AAV-shFABP5 compared to shControl MSNs (two-way ANOVA, $F_{(19, 684)} = 165.6$, $p<0.0001$). Posthoc testing revealed that at the middle range of current steps, the inter-spike intervals were increased resulting in reduced instantaneous firing frequency in MSNs expressing AAV-shFABP5 compared to shControl MSNs (t=2.105; df=720, $p=0.036$ with posthoc Fisher's LSD test for firing train evoked with 70 pA current step; Figure 8A and C). Further analysis of active and passive MSN electrical properties showed that FABP5 knockdown led to a more depolarized resting membrane potential (t=2.959; df=37, $p=0.005$, Table 1) and increased membrane capacitance (t=2.175; df=29, $p=0.038$, Table 1). Other properties, such as action potential voltage and current threshold and input resistance were unchanged in AAV-sh-FABP5 MSNs (Table 1). Overall, FABP5 knockdown in the NAcSh

modulates MSN intrinsic excitability, but had no effect on spontaneous glutamatergic synaptic transmission.

4. Discussion

We first conducted a topographic transcriptomic analysis of the adult male mouse NAcSh in order to identify novel pathways with targets for future pharmacotherapeutic development for cocaine use disorder. This approach clearly identified retinoic acid signaling. FABP5 was identified by both the current and previous topographic transcriptomic analyses, showed selective expression in the NAcSh, and is an important retinoic acid binding partner. Therefore, we knocked down expression of the NAcSh-enhanced retinoic acid binding partner FABP5 in the NAcSh of rats via an adeno-associated viral vector. Rats with FABP5 knockdown in the NAcSh showed decreased cocaine taking behavior compared to control rats and showed correlative alterations in intrinsic excitability of MSNs, the major population of cells and the only output of the NAcSh. Thus, retinoic acid signaling was confirmed as an important pathway in the NAcSh for the regulation of cocaine-seeking behaviors.

This unbiased topographic transcriptomic analysis would not be possible without the genome-wide database of *in situ* hybridization data from the Allen Brain Institute. However, a caveat of this paper is that the atlas of brain tissue is from mice while the FABP5 knockdown behavior and electrophysiological experiments were conducted in rats. Available evidence shows that regional gene expression is conserved from mice to humans, and thus should be conserved between mice and rats (Strand et al., 2007), although validation of the enrichment of FABP5 in the rat NAcSh is needed. Despite the differences in species, we were able to identify the pathway with the topographic transcriptomics and when manipulated in rats, caused a decrease in cocaine taking behaviors and MSN activity. This cross-species study provides some confidence that retinoic acid signaling will prove important for drug taking behaviors in humans. Additionally, the atlas contains data only from male mice and the behavior and electrophysiological experiments were conducted only in male rats. For a more complete understanding of the role of FABP5 in the nucleus accumbens, future studies on female animals are necessary.

Our previous topographic analysis of the NAcSh (Zhang et al., 2016a) used the Anatomic Gene Expression Atlas (AGEA) tool of the Allen Brain Atlas (Ng et al., 2009) which utilizes a seed voxel to identify transcripts with expression near the seed voxel, whereas the current project used a novel two-step analysis first identifying five seed transcripts from the AGEA and then using the Allen Brain Atlas' correlation feature to identify transcripts with similar expression patterns in the striatum. The previous AGEA analysis (Zhang et al., 2016a) utilized expression data for only 4,376 coronally-available transcripts to identify 176 NAcSh-enhanced transcripts while the current two-step strategy searched and analyzed data from >20,000 transcripts to identify 1,426 transcripts matching at least three of the five seed transcripts. The prior analysis narrowly failed to identify the canonical *RAR Signaling* pathway with a $-\log(p) = 1.2$ while the current analysis produced a significant $-\log(p) = 1.4$.

The current procedure identified many more targets than the previous AGEA analysis, but these targets were largely not overlapping. Less than half (64 of 176) of the transcripts identified in the AGEA analysis were identified by the current analysis. Conversely, the AGEA analysis also failed to identify many NAcSh-enhanced transcripts from the current analysis. Our conclusion is that both analyses have significant Type II error and thus the two different strategies are complementary. As an example, Slit2 was only identified as NAcSh-enhanced in the current analysis yet its signaling partner Robo1 was only identified by the AGEA analysis, demonstrating the complementary nature of the different approaches.

One rationale for the current two-step strategy was to be able to identify novel NAcSh-enhanced transcripts from sagittal experiments not available to the coronal-limited AGEA analysis. While the current strategy identified hundreds of sagittal NAcSh-enhanced transcripts, it was unable to identify two previously manually identified retinoic acid-related transcripts (RBP1 and RDH10) enhanced in the NAcSh. Both targets only had a significant correlation with one of the seeds (STRA6), but our strategy required significant correlations with three seeds to be significant. Additionally, the previous analysis relies on the accuracy and uniformity of all brain slices, precise alignment of each voxel between animals, and the results can depend greatly on the specific voxel selected. Our conclusion is that the two-step procedure is an improvement over the previous one-step, but still does not produce an exhaustive list of NAcSh-enhanced transcripts.

Although FABP5 knockdown in the NAcSh altered cocaine taking, knockdown rats did not show previous alterations in anxiety-like or depression-like behaviors (Zhang et al., 2019). A likely explanation for a lack of effect of FABP5 knockdown on anxiety- and depression-like behaviors is that the other retinoic acid binding partner, CRABP2, or some other mechanism, partially compensated for the loss of FABP5. RA signaling does have demonstrated downstream effects on transcription through PPARD (via FABP5) but also through RARs (via CRABP2) (Schug et al., 2007). Perhaps RA signaling via CRABP2/RARs compensated for the loss of FABP5 in the spontaneous anxiety- and depression-like tests, but not when challenged by high exposure to cocaine as in self-administration tests. However, we have recently shown that knockdown of CRABP2, but not knockdown of FABP5, is able to alter anxiety- and depression-like behavior (Zhang et al., 2019). These two binding partners may therefore differentially regulate the behavioral results of RA signaling in the NAcSh. Further investigation is needed to understand the downstream effects of these two binding partners and their relative contributions to addiction-related behaviors.

The results of the electrophysiological studies shown here provide an overall assessment of the global consequences of decreased FABP5 on NAcSh MSN activity in the absence of cocaine. This preliminary assessment suggests altered neuronal function that may be in place prior to cocaine self-administration and may contribute to the mechanism underlying the reduced cocaine-taking behaviors. Silencing FABP5 had no effect on either frequency or amplitude of spontaneous glutamatergic synaptic currents indicating that receptors and/or ion channels that mediate excitatory transmission at both pre- and postsynaptic sites are not downstream targets of FABP5. This result is somewhat puzzling given the reported role of the RA pathway in regulating AMPA-receptor mediated synaptic transmission and synaptic plasticity (Aoto et al., 2008; Arendt et al., 2015; Hsu et al., 2019; Loweth et al., 2019).

Changes in synaptic transmission upon FABP5 silencing might occur as an initial insult, but then be compensated by altered neuronal firing (from MSNs observed in the present study and/or other neuronal subtypes in the NAcSh) to maintain global neuronal activity within a physiological range. Alternatively, an increase in synaptic strength might develop later as part of a cell-autonomous homeostatic loop in response to the global decrease in excitability induced by silencing FABP5.

The changes in intrinsic excitability induced by FABP5 knockdown are complex. The total number of evoked action potentials and the interspike interval decreased at the middle range of stimulating current steps while a significant increase of MSN firing was evoked with injected current of high intensity in the FABP5 knockdown group when cells were maintained at the same baseline of −70mV. Moreover, the resting membrane potential was also more depolarized as well as membrane capacitance was significantly higher compared to control in AAV-shFABP5 MSNs while membrane resistance was not significantly different. These results indicate that FABP5 in the male nucleus accumbens may play a role in the intrinsic excitability of MSNs, but more extensive analysis is necessary to resolve the mechanisms of these complex results. For example, increased membrane capacitance suggests a larger soma or other morphological alterations in MSNs due to FABP5 knockdown. It is critical to mention that *in vivo* striatal MSNs can have large changes in the resting membrane potential driven by glutamatergic cortical inputs; resting at hyperpolarized potentials without stimulation (−85mV, “down-state”) and shift to more depolarized potentials (−55mV, “up-state”) with stimulation from cortical afferents (Wickens and Wilson, 1998; Surmeier et al., 2007). FABP5 knockdown MSNs have a more depolarized RMP (average −66mV) compared to control MSNs (average −79mV), suggesting that FABP5 knockdown could favor transition of MSNs to the “up-state”. Yet, further experiments are needed to examine this hypothesis. It has been previously shown that members of FABPs family are coupled with Na+/K+-ATPase which, in turn, due to its electrogenic properties is known to contribute to the resting membrane potential and electrical cell capacitance (Incerpi et al., 1992; Lu et al., 1995; Sokolov et al., 1998; Su et al., 2016). Moreover, Na+/K+-ATPase is important for the modulation of neuronal repetitive firing, in particular via regulation of A-type K+ channel activity (Botta et al., 2010; Zhang et al., 2015). Finally, recently it has been found that Na+/K+ATPase plays a role in cocaine addiction and is critical for striatal and, in particular, NAc function (Mackler et al., 1998; Wu et al., 2007; Kurauchi et al., 2019). Based on this, modulation of Na+/K+-ATPase activity may be one of the potential mechanisms by which downregulation of FABP5 alters MSNs intrinsic excitability, however future work is necessary to explore the role of K+ channels or other voltage channels on the effects seen here and to fully understand the role of FABP5 in MSN intrinsic excitability.

Another important aspect that requires further investigation is how FABP5 silencing would affect synaptic transmission and neuronal excitability in NAc MSNs from rats that self-administer cocaine, especially in a context of D1-MSN and D2-MSN specific mechanisms since both are known to be involved in regulating cocaine taking behavior (Surmeier et al., 2007; Lobo and Nestler, 2011; Smith and Robbins, 2013). The current FABP5 knockdown method is not targeted to any one cell type of the NAcSh as the AAV2 serotype is not specific to any one neuronal subtype. As the electrophysiological analysis is correlated with

the cocaine self-administration it is difficult to predict the effects of this decrease in intrinsic excitability on the output of the NAc. However, as retinoic acid signaling is important for neuronal development and regulation and there is some evidence for a role of retinoic acid in the regulation of dendritic morphology (Maden, 2007; Liu et al., 2008; Rhinn and Dollé, 2012), future examination of the role of FABP5 on MSN dendritic morphology is critical. Additionally, future work is needed to confirm whether electrophysiological changes seen here 3 weeks post viral injection are maintained at 9 weeks post viral injection (when cocaine self-administration commenced in this study). This preliminary investigation has prompted several hypotheses but extensive electrophysiological investigation is needed to fully examine the role of FABP5 in MSN intrinsic excitability.

The current results suggest inhibition of FABP5 may be a promising therapeutic target for cocaine use disorder. Knockdown of FABP5 in the NAcSh caused a rightward shift in the ascending limb of the dose response function, indicating an elevation in the threshold of reinforcement for cocaine. Although we did not find significant effects of FABP5 knockdown on reinstatement of cocaine, our procedure was a within-session reinstatement with rats having access to cocaine in the same session. We did not assess effects of FABP5 knockdown on cocaine-induced reinstatement after a prolonged period of abstinence, which would more closely resemble a treatment-seeking individual with cocaine use disorder. Future studies should therefore examine the role of FABP5 on between-session reinstatement or cue reactivity following long-term abstinence via shRNA knockdown of FABP5 as well as small molecule inhibitors of FABP5.

4.1 Conclusions

The two-step topographic transcriptomic analysis of the male NAcSh identified RA signaling as a possible promising treatment target for cocaine use disorder; manipulation of FABP5 provides causal evidence that retinoic acid signaling is indeed a promising strategy for cocaine use disorder. Taken together, modulating RA signaling, potentially through inhibition of FABP5, could be a potent therapeutic for treatment-seeking individuals with cocaine use disorder. To aid pharmacotherapeutic development for cocaine use disorder, further investigation should focus on understanding the genomic and non-genomic roles of retinoic acid signaling on cocaine taking behaviors and activity of medium spiny neurons in the NAcSh.

Supplementary Material

Refer to Web version on PubMed Central for supplementary material.

Funding and Disclosure

Funding was provided by National Institutes of Health [DA047102 (TAG, FL), DA029091 (TAG), ES007254 (CMT), DA007287 (EJC)], and the UTMB Presidential Scholars Program (CMT). The authors declare no conflict of interest.

Bibliography

Aoto J, Nam CI, Poon MM, Ting P, Chen L (2008) Synaptic signaling by all-trans retinoic acid in homeostatic synaptic plasticity. Neuron 60:308–320. [PubMed: 18957222]

Arendt KL, Zhang Y, Jurado S, Malenka RC, Sudhof TC, Chen L (2015) Retinoic Acid and LTP Recruit Postsynaptic AMPA Receptors Using Distinct SNARE-Dependent Mechanisms. Neuron 86:442–456. [PubMed: 25843403]

Balmer JE, Blomhoff R (2002) Gene expression regulation by retinoic acid. Journal of lipid research 43:1773–1808. [PubMed: 12401878]

Barrot M, Olivier JD, Perrotti LI, DiLeone RJ, Berton O, Eisch AJ, Impey S, Storm DR, Neve RL, Yin JC, Zachariou V, Nestler EJ (2002) CREB activity in the nucleus accumbens shell controls gating of behavioral responses to emotional stimuli. Proc Natl Acad Sci U S A 99:11435–11440. [PubMed: 12165570]

Benzon C, Johnson S, McCue D, Li D, Green T, Hommel J (2014) Neuromedin U receptor 2 knockdown in the paraventricular nucleus modifies behavioral responses to obesogenic high-fat food and leads to increased body weight. Neuroscience 258:270–279. [PubMed: 24269937]

Bilbao A, Rieker C, Cannella N, Parlato R, Golda S, Piechota M, Korostynski M, Engblom D, Przewlocki R, Schutz G, Spanagel R, Parkitna JR (2014) CREB activity in dopamine D1 receptor expressing neurons regulates cocaine-induced behavioral effects. Frontiers in behavioral neuroscience 8:212. [PubMed: 24966820]

Botta P, de Souza FMS, Sangrey T, De Schutter E, Valenzuela CF (2010) Alcohol excites cerebellar Golgi cells by inhibiting the Na+/K+ ATPase. Neuropsychopharmacology : official publication of the American College of Neuropsychopharmacology 35:1984–1996. [PubMed: 20520600]

Chen L, Lau AG, Sarti F (2014) Synaptic retinoic acid signaling and homeostatic synaptic plasticity. Neuropharmacology 78:3–12. [PubMed: 23270606]

Crofton EJ, Nenov MN, Zhang Y, Scala F, Page SA, McCue DL, Li D, Hommel JD, Laezza F, Green TA (2017) Glycogen synthase kinase 3 beta alters anxiety-, depression-, and addiction-related behaviors and neuronal activity in the nucleus accumbens shell. Neuropharmacology 117:49–60. [PubMed: 28126496]

Dong Y, Green T, Saal D, Marie H, Neve R, Nestler EJ, Malenka RC (2006) CREB modulates excitability of nucleus accumbens neurons. Nature neuroscience 9:475–477. [PubMed: 16520736]

Douglass J, Daoud S (1996) Characterization of the human cDNA and genomic DNA encoding CART: a cocaine-and amphetamine-regulated transcript. Gene 169:241–245. [PubMed: 8647455]

Douglass J, McKinzie AA, Couceyro P (1995) PCR differential display identifies a rat brain mRNA that is transcriptionally regulated by cocaine and amphetamine. Journal of Neuroscience 15:2471–2481. [PubMed: 7891182]

Duester G (2008) Retinoic acid synthesis and signaling during early organogenesis. Cell 134:921–931. [PubMed: 18805086]

Green TA, Alibhai IN, Unterberg S, Neve RL, Ghose S, Tamminga CA, Nestler EJ (2008) Induction of activating transcription factors (ATFs) ATF2, ATF3, and ATF4 in the nucleus accumbens and their regulation of emotional behavior. The Journal of Neuroscience 28:2025–2032. [PubMed: 18305237]

Green TA, Alibhai IN, Hommel JD, DiLeone RJ, Kumar A, Theobald DE, Neve RL, Nestler EJ (2006) Induction of inducible cAMP early repressor expression in nucleus accumbens by stress or amphetamine increases behavioral responses to emotional stimuli. The Journal of neuroscience : the official journal of the Society for Neuroscience 26:8235–8242.

Green TA, Alibhai IN, Roybal CN, Winstanley CA, Theobald DE, Birnbaum SG, Graham AR, Unterberg S, Graham DL, Vialou V, Bass CE, Terwilliger EF, Bardo MT, Nestler EJ (2010) Environmental enrichment produces a behavioral phenotype mediated by low cyclic adenosine monophosphate response element binding (CREB) activity in the nucleus accumbens. Biological psychiatry 67:28–35. [PubMed: 19709647]

Hommel JD, Sears RM, Georgescu D, Simmons DL, DiLeone RJ (2003) Local gene knockdown in the brain using viral-mediated RNA interference. Nature medicine 9:1539–1544.

Hsu YT, Li J, Wu D, Sudhof TC, Chen L (2019) Synaptic retinoic acid receptor signaling mediates mTOR-dependent metaplasticity that controls hippocampal learning. Proc Natl Acad Sci U S A 116:7113–7122. [PubMed: 30782829]

Incerpi S, Jefferson JR, Wood WG, Ball WJ, Schroeder F (1992) Na pump and plasma membrane structure in L-cell fibroblasts expressing rat liver fatty acid binding protein. Archives of biochemistry and biophysics 298:35–42. [PubMed: 1326253]

Kane MA, Folias AE, Wang C, Napoli JL (2008) Quantitative profiling of endogenous retinoic acid in vivo and in vitro by tandem mass spectrometry. Analytical chemistry 80:1702–1708. [PubMed: 18251521]

Kurauchi Y, Yoshimaru Y, Kajiwara Y, Yamada T, Matsuda K, Hisatsune A, Seki T, Katsuki H (2019) Na+, K+-ATPase inhibition causes hyperactivity and impulsivity in mice via dopamine D2 receptor-mediated mechanism. Neuroscience research 146:54–64. [PubMed: 30296459]

Larson EB, Graham DL, Arzaga RR, Buzin N, Webb J, Green TA, Bass CE, Neve RL, Terwilliger EF, Nestler EJ, Self DW (2011) Overexpression of CREB in the nucleus accumbens shell increases cocaine reinforcement in self-administering rats. The Journal of neuroscience : the official journal of the Society for Neuroscience 31:16447–16457. [PubMed: 22072694]

Liu Y, Kagechika H, Ishikawa J, Hirano H, Matsukuma S, Tanaka K, Nakamura S (2008) Effects of retinoic acids on the dendritic morphology of cultured hippocampal neurons. Journal of neurochemistry 106:1104–1116. [PubMed: 18466335]

Lobo MK, Nestler EJ (2011) The striatal balancing act in drug addiction: distinct roles of direct and indirect pathway medium spiny neurons. Frontiers in neuroanatomy 5:41. [PubMed: 21811439]

Loweth JA, Reimers JM, Caccamise A, Stefanik MT, Woo KKY, Chauhan NM, Werner CT, Wolf ME (2019) mGlu1 tonically regulates levels of calcium-permeable AMPA receptors in cultured nucleus accumbens neurons through retinoic acid signaling and protein translation. European Journal of Neuroscience 50:2590–2601.

Lu C-C, Kabakov A, Markin VS, Mager S, Frazier GA, Hilgemann DW (1995) Membrane transport mechanisms probed by capacitance measurements with megahertz voltage clamp. Proceedings of the National Academy of Sciences 92:11220–11224.

Mackler SA, Kleyman TR, Cha X-Y (1998) Regulation of the Na+/K+-ATPase Pumpin Vitro after Long-Term Exposure to Cocaine: Role of Serotonin. Journal of Pharmacology and Experimental Therapeutics 285:835–843.

Maden M (2007) Retinoic acid in the development, regeneration and maintenance of the nervous system. Nature Reviews Neuroscience 8:755–765. [PubMed: 17882253]

McClung CA, Nestler EJ (2003) Regulation of gene expression and cocaine reward by CREB and DeltaFosB. Nature neuroscience 6:1208–1215. [PubMed: 14566342]

McKinzie D, Rodd-Henricks Z, Dagon C, Murphy J, McBride W (1999) Cocaine Is Self-administered into the Shell Region of the Nucleus Accumbens in Wistar Rats. Annals of the New York Academy of Sciences 877:788–791. [PubMed: 10415705]

McMahon LR, Cunningham KA (1999) Antagonism of 5-hydroxytryptamine4 receptors attenuates hyperactivity induced by cocaine: putative role for 5-hydroxytryptamine4 receptors in the nucleus accumbens shell. Journal of Pharmacology and Experimental Therapeutics 291:300–307.

Ng L, Bernard A, Lau C, Overly CC, Dong HW, Kuan C, Pathak S, Sunkin SM, Dang C, Bohland JW, Bokil H, Mitra PP, Puelles L, Hohmann J, Anderson DJ, Lein ES, Jones AR, Hawrylycz M (2009) An anatomic gene expression atlas of the adult mouse brain. Nature neuroscience 12:356–362. [PubMed: 19219037]

Niewiadomska-Cimicka A, Krzyżosiak A, Ye T, Podleśny-Drabiniok A, Dembélé D, Dollé P, Krężel W (2017) Genome-wide analysis of RARβ transcriptional targets in mouse striatum links retinoic acid signaling with Huntington's disease and other neurodegenerative disorders. Molecular neurobiology 54:3859–3878. [PubMed: 27405468]

Pliakas AM, Carlson RR, Neve RL, Konradi C, Nestler EJ, Carlezon WA Jr. (2001) Altered responsiveness to cocaine and increased immobility in the forced swim test associated with elevated cAMP response element-binding protein expression in nucleus accumbens. The Journal of neuroscience : the official journal of the Society for Neuroscience 21:7397–7403. [PubMed: 11549750]

Pontieri FE, Tanda G, Di Chiara G (1995) Intravenous cocaine, morphine, and amphetamine preferentially increase extracellular dopamine in the "shell" as compared with the "core" of the rat nucleus accumbens. Proc Natl Acad Sci U S A 92:12304–12308. [PubMed: 8618890]

Rhinn M, Dollé P (2012) Retinoic acid signalling during development. Development 139:843–858. [PubMed: 22318625]

Scala F, Nenov MN, Crofton EJ, Singh AK, Folorunso O, Zhang Y, Chesson BC, Wildburger NC, James TF, Alshammari MA (2018) Environmental enrichment and social isolation mediate neuroplasticity of medium spiny neurons through the GSK3 pathway. Cell reports 23:555–567. [PubMed: 29642012]

Schug TT, Berry DC, Shaw NS, Travis SN, Noy N (2007) Opposing effects of retinoic acid on cell growth result from alternate activation of two different nuclear receptors. Cell 129:723–733. [PubMed: 17512406]

Smith DG, Robbins TW (2013) The neurobiological underpinnings of obesity and binge eating: a rationale for adopting the food addiction model. Biological psychiatry 73:804–810. [PubMed: 23098895]

Sokolov VS, Stukolov S, Darmostuk A, Apell H-J (1998) Influence of sodium concentration on changes of membrane capacitance associated with the electrogenic ion transport by the Na, K-ATPase. European biophysics journal 27:605–617. [PubMed: 9791943]

Strand AD, Aragaki AK, Baquet ZC, Hodges A, Cunningham P, Holmans P, Jones KR, Jones L, Kooperberg C, Olson JM (2007) Conservation of regional gene expression in mouse and human brain. PLoS Genet 3:e59. [PubMed: 17447843]

Su X, Tan QS, Parikh BH, Tan A, Mehta MN, Wey YS, Tun SBB, Li L-J, Han X-Y, Wong TY (2016) Characterization of fatty acid binding protein 7 (FABP7) in the murine retina. Investigative ophthalmology & visual science 57:3397–3408. [PubMed: 27367508]

Surmeier DJ, Ding J, Day M, Wang Z, Shen W (2007) D1 and D2 dopamine-receptor modulation of striatal glutamatergic signaling in striatal medium spiny neurons. Trends in neurosciences 30:228–235. [PubMed: 17408758]

Thompson CL, Ng L, Menon V, Martinez S, Lee C-K, Glattfelder K, Sunkin SM, Henry A, Lau C, Dang C (2014) A high-resolution spatiotemporal atlas of gene expression of the developing mouse brain. Neuron 83:309–323. [PubMed: 24952961]

Wallace DL, Vialou V, Rios L, Carle-Florence TL, Chakravarty S, Kumar A, Graham DL, Green TA, Kirk A, Iniguez SD (2008) The influence of ΔFosB in the nucleus accumbens on natural reward-related behavior. The Journal of Neuroscience 28:10272–10277. [PubMed: 18842886]

Wallace DL, Han MH, Graham DL, Green TA, Vialou V, Iniguez SD, Cao JL, Kirk A, Chakravarty S, Kumar A, Krishnan V, Neve RL, Cooper DC, Bolanos CA, Barrot M, McClung CA, Nestler EJ (2009) CREB regulation of nucleus accumbens excitability mediates social isolation-induced behavioral deficits. Nature neuroscience 12:200–209. [PubMed: 19151710]

Wickens J, Wilson C (1998) Regulation of action-potential firing in spiny neurons of the rat neostriatum in vivo. Journal of neurophysiology 79:2358–2364. [PubMed: 9582211]

Wu Z-Q, Chen J, Chi Z-Q, Liu J-G (2007) Involvement of dopamine system in regulation of Na+, K+-ATPase in the striatum upon activation of opioid receptors by morphine. Molecular pharmacology 71:519–530. [PubMed: 17068092]

Zhang H-Y, Picton L, Li W-C, Sillar KT (2015) Mechanisms underlying the activity-dependent regulation of locomotor network performance by the Na+ pump. Scientific reports 5:16188. [PubMed: 26541477]

Zhang Y, Crofton EJ, Smith TE, Koshy S, Li D, Green TA (2019) Manipulation of retinoic acid signaling in the nucleus accumbens shell alters rat emotional behavior. Behavioural brain research 376:112177. [PubMed: 31449909]

Zhang Y, Crofton EJ, Li D, Lobo MK, Fan X, Nestler EJ, Green TA (2014) Overexpression of DeltaFosB in nucleus accumbens mimics the protective addiction phenotype, but not the protective depression phenotype of environmental enrichment. Frontiers in behavioral neuroscience 8.

Zhang Y, Kong F, Crofton EJ, Dragosljvich SN, Sinha M, Li D, Fan X, Koshy S, Hommel JD, Spratt HM (2016a) Transcriptomics of Environmental Enrichment Reveals a Role for Retinoic Acid Signaling in Addiction. Frontiers in molecular neuroscience 9.

Zhang Y, Crofton EJ, Fan X, Li D, Kong F, Sinha M, Luxon BA, Spratt HM, Lichti CF, Green TA (2016b) Convergent transcriptomics and proteomics of environmental enrichment and cocaine

identifies novel therapeutic strategies for addiction. Neuroscience 339:254–266. [PubMed: 27717806]

Highlights:

- Analysis identifies transcripts with enhanced expression in nucleus accumbens shell
- Retinoic acid signaling pathway is overrepresented in shell specific transcripts
- Reducing RA signaling member FABP5 in rat shell reduces cocaine self-administration
- Shell knockdown of FABP5 modulates intrinsic excitability of medium spiny neurons
- RA signaling and FABP5 are validated as avenue for pharmacotherapeutic development

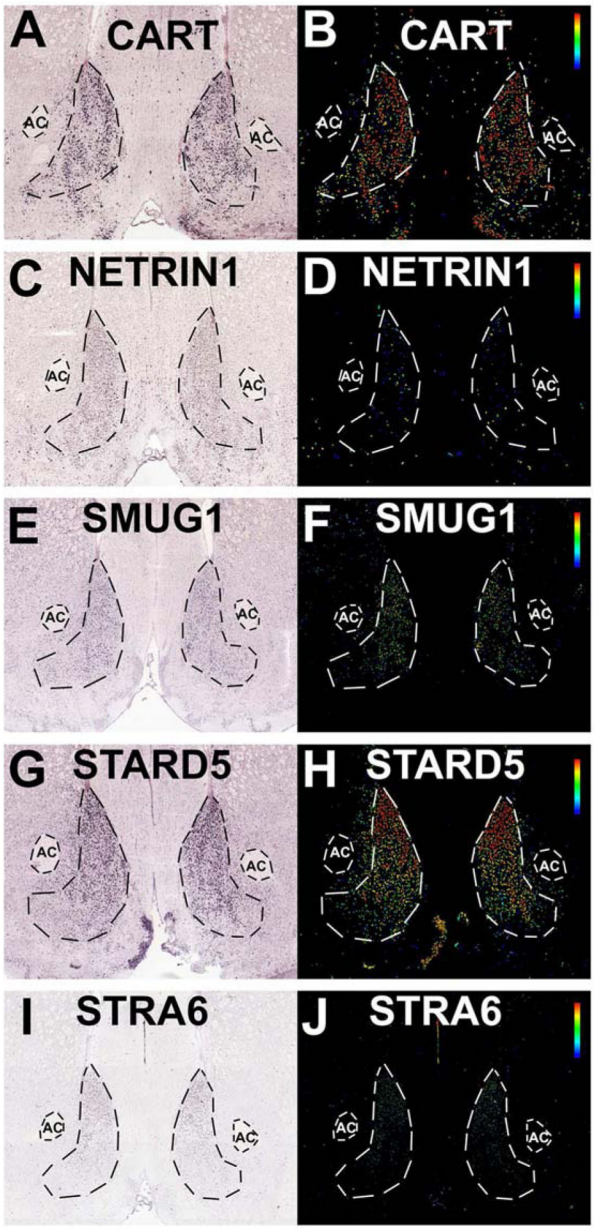

Figure 1: Seed transcripts with NAcSh specific expression used for topographic transcriptomic analysis.

In situ hybridization (left) and expression (right) images from the Allen Brain Atlas for cocaine and amphetamine regulated transcript (CART, Panels A-B), netrin1 (C-D), single strand-selective monofunctional uracil-DNA glycosylase 1 (SMUG1, Panels E-F), StAR related lipid transfer domain containing 5 (STARD5, Panels G-H), stimulated by retinoic acid 6 (STRA6, Panels I-J). CART: http://mouse.brain-map.org/experiment/show/72077479, NTN1: http://mouse.brain-map.org/experiment/show/74511838, SMUG1: http://mouse.brain-map.org/experiment/show/73992919, STARD5: http://mouse.brain-map.org/experiment/show/70813909, STRA6: http://mouse.brain-map.org/experiment/show/75041492.

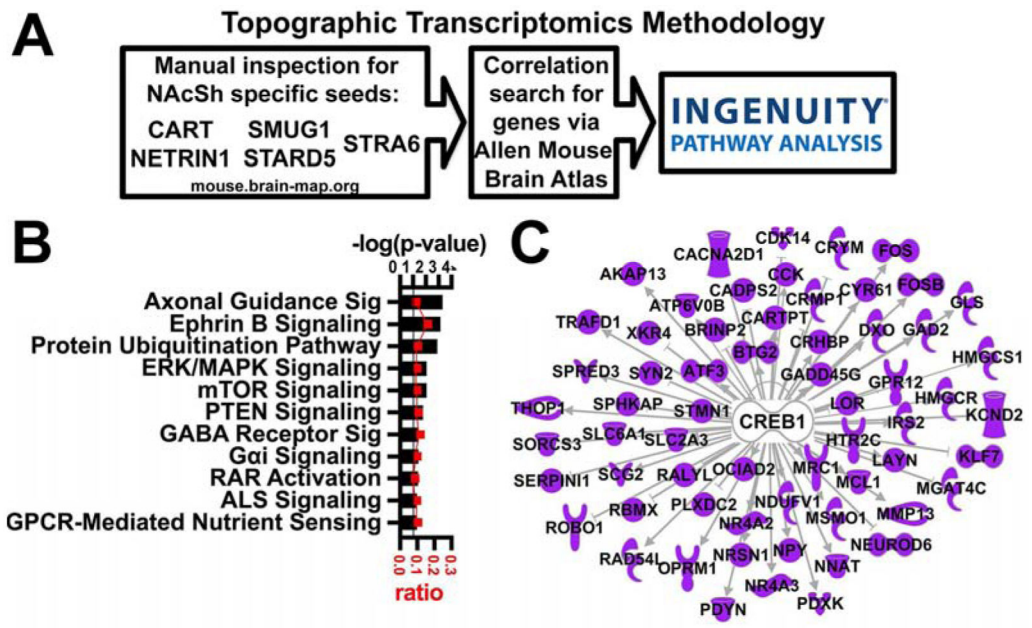

Figure 2: Topographic transcriptomic analysis of the nucleus accumbens shell.

A. Overview of topographic transcriptomics methodology. B. A selection of significant Canonical Pathways. Horizontal axis (bars) represents −log (*p*-value) and ratio (red squares) of NAcSh transcripts to all transcripts in the pathway. Black line represents threshold $p = 0.05$. C. CREB is identified as an upstream regulator.

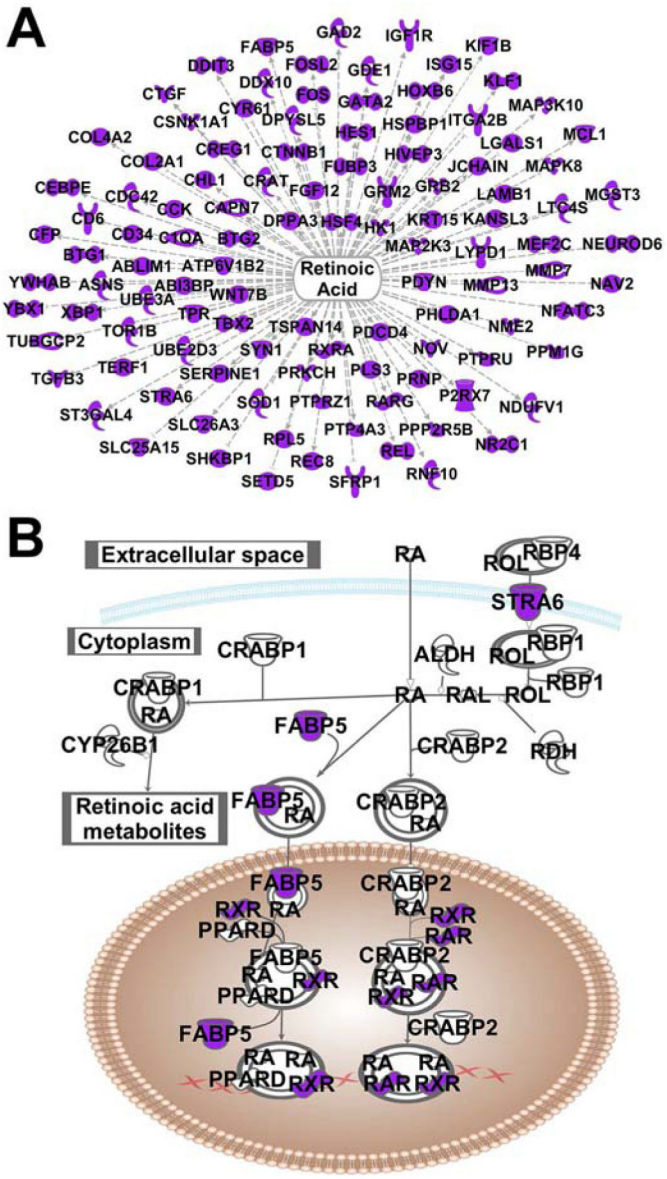

Figure 3. Retinoic acid signaling pathway is identified by topographic transcriptomic analysis of NAcSh.

A. Retinoic acid (tretinoin) is identified as an upstream regulator. B. Core retinoic acid signaling pathway overlaid with transcripts identified in the topographic transcriptomic analysis (purple symbols).

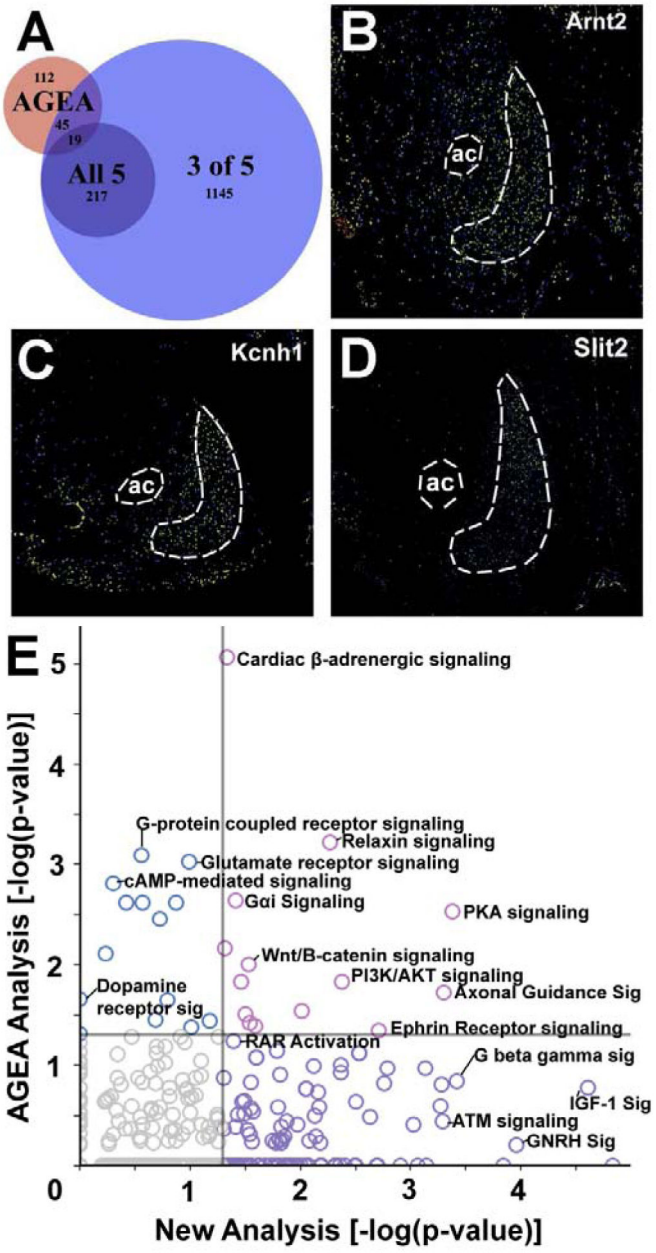

Figure 4. Comparison of previous AGEA analysis vs. current analysis and novel results.

A. Venn diagram showing the intersection of NAcSh-enhanced transcripts from the previous AGEA analysis with the current analysis. The large blue circle represents significant results from the 1,426 transcripts with significant correlation to three of the five seed transcripts (criteria for "NAcSh-enhanced"). The smaller purple circle is the set of transcripts that had significant correlations with all five seed genes. B - D. Allen brain atlas expression images for NAcSh-enhanced targets not identified by the previous AGEA analysis: B. Arnt2 http://mouse.brain-map.org/experiment/show/71358590, C. Kcnh1 http://mouse.brain-map.org/experiment/show/73636099, and D. Slit2 http://mouse.brain-map.org/experiment/show/79591683. ac = anterior commissure. NAcSh and AC are outlined. E. Scatterplot of −log(p-

values) from an IPA analysis of overrepresented canonical pathways from the current analysis (X axis) vs. the previous AGEA analysis (Y axis). Gray vertical and horizontal lines represent statistical significance ($p < 0.05$) and symbol colors indicate significant pathways in previous analysis (blue), current analysis (purple), and both analyses (pink).

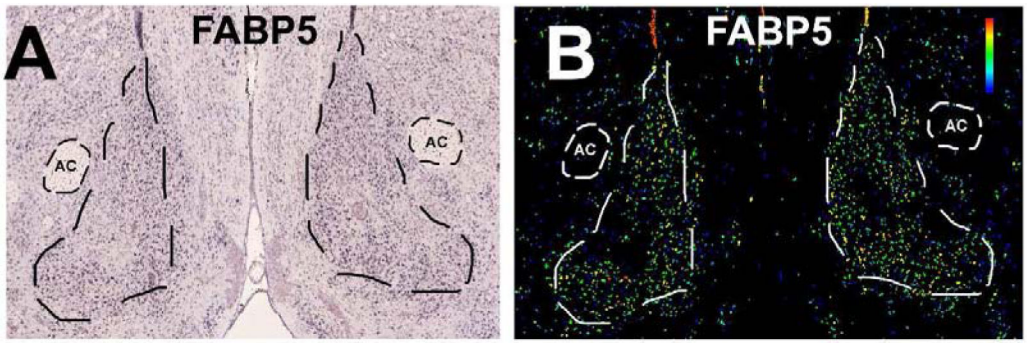

Figure 5. Fatty acid binding protein 5 (FABP5), an RA signaling pathway transcript, shows enhanced expression in the NAcSh.

In situ hybridization (A) and expression (B) images from the Allen Brain Atlas for fatty acid binding protein 5 (FABP5) (http://mouse.brain-map.org/experiment/show/70634396).

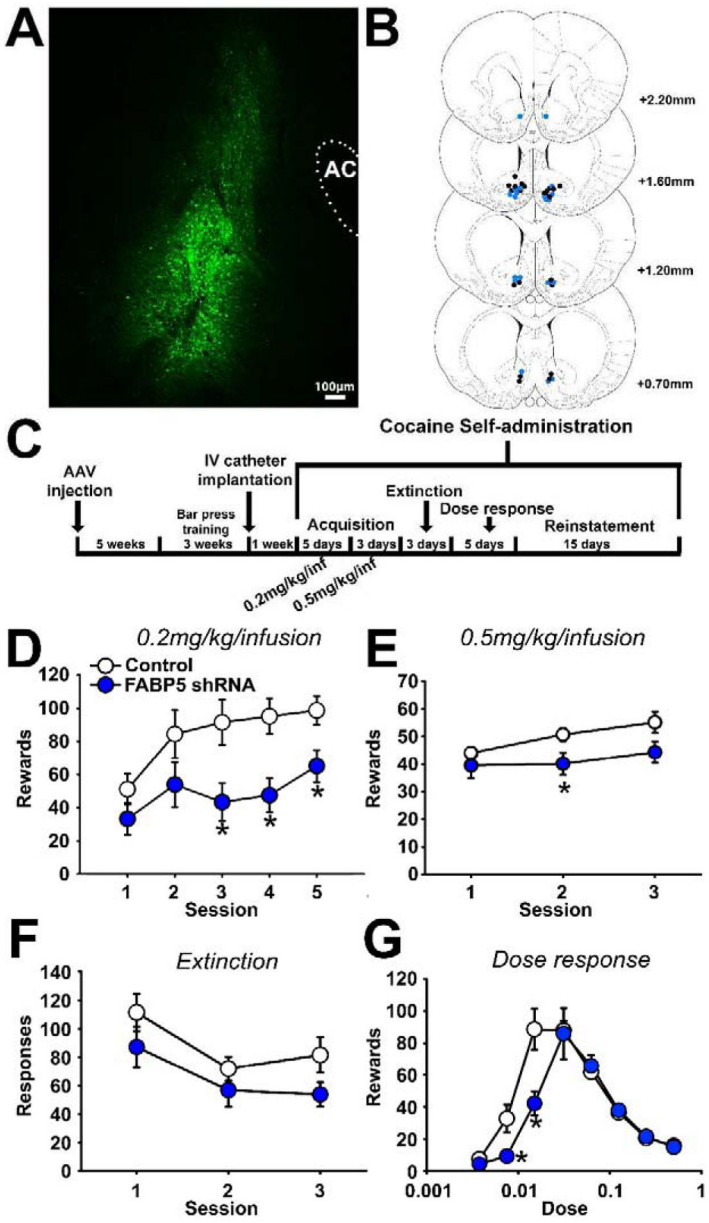

Figure 6. Knockdown of fatty acid binding protein 5 (FABP5) in the rat NAcSh decreases cocaine self-administration.

A. Representative immunofluorescence (eGFP) of viral vector in the NAcSh (AC=anterior commissure). B. Placement of AAV injections for control vector (black) or shFABP5 knockdown (blue) for cocaine self-administration. (C) Diagram of cocaine self-administration methods. Acquisition at 0.2 mg/kg/infusion (D) and 0.5 mg/kg/infusion (E), extinction (F), and dose response (G) of cocaine self-administration in control or FABP5 knockdown rats.

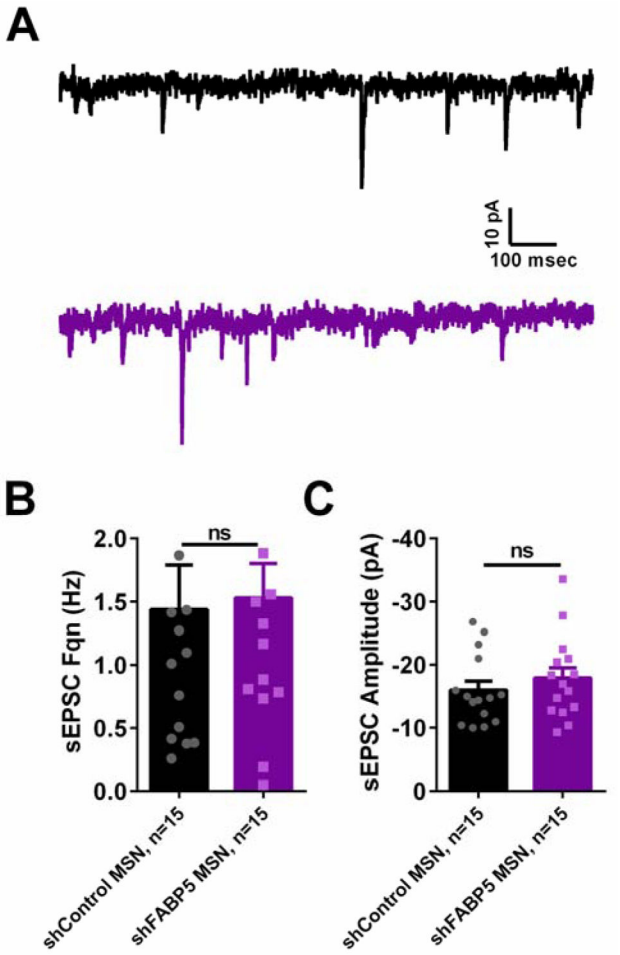

Figure 7. FABP5 knockdown does not affect spontaneous excitatory glutamatergic synaptic transmission in rat NAcSh MSNs.

A. Representative traces showing sEPSCs recorded from MSNs transfected with AAV-shControl (black trace, top) or AAV-shFABP5 (purple trace, bottom). FABP5 knockdown does not affect sEPSC frequency (B) or sEPSC amplitude (C). ns – not significant with Student's t-test, $p>0.05$. "n" represents number of recorded MSNs.

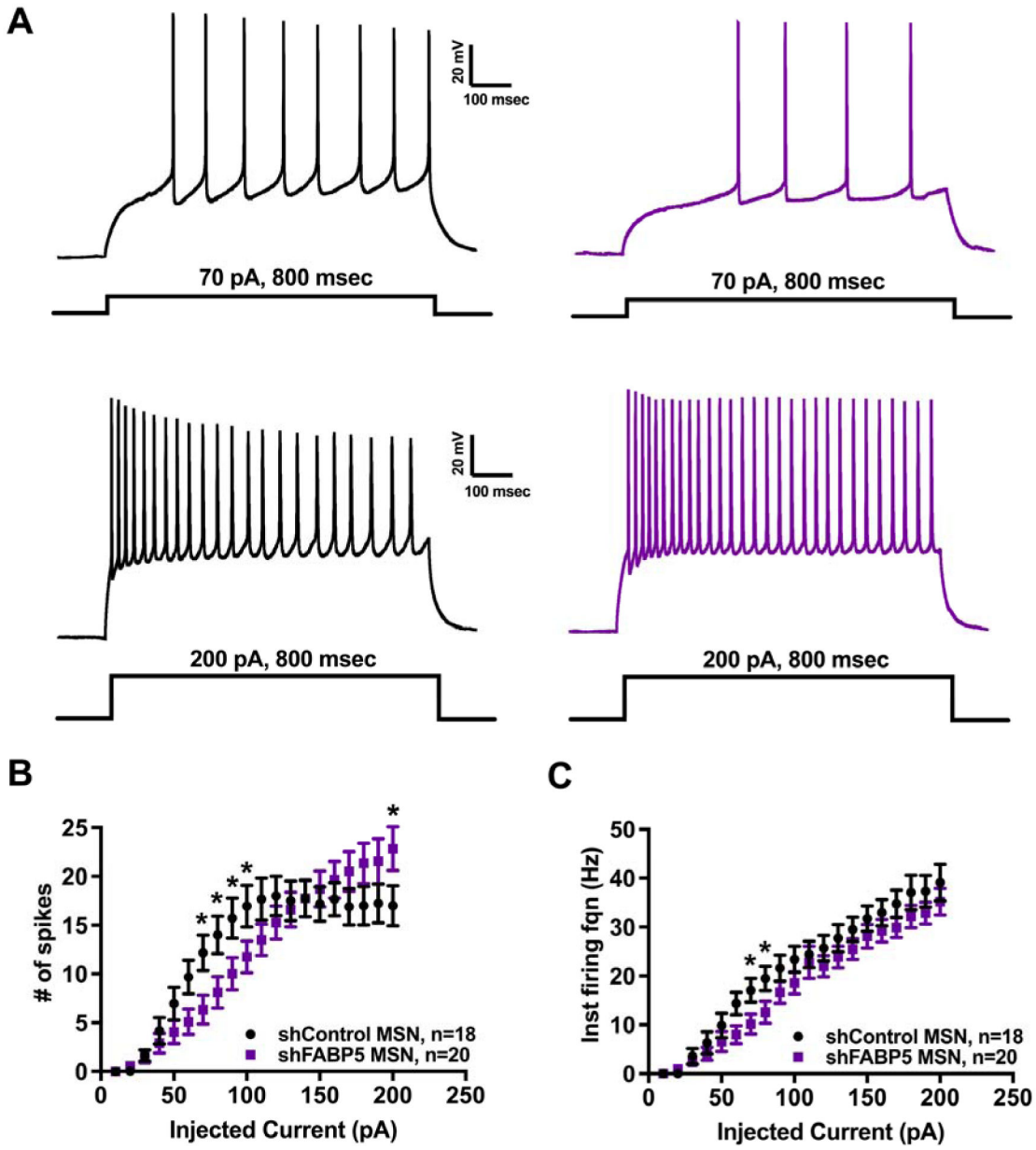

Figure 8. FABP5 knockdown modulates NAcSh MSNs intrinsic excitability.

A. Representative traces showing train of evoked action potentials at 70 pA current step (upper traces) and 200 pA current step (lower traces) recorded from MSNs transfected with AAV-shControl (black traces, left) or AAV-shFABP5 (purple traces, right). B. Input-output curve showing significant reduction of evoked action potential firing in the middle range of stimuli intensity along with an increase in firing at high stimulus in FABP5 knockdown MSNs. C. Input-output curve showing significant reduction of instantaneous firing frequency in the middle range of stimuli intensity in FABP5 knockdown MSNs. *$p<0.05$ with two-way repeated measures ANOVA and posthoc Fisher's LSD test. "n" represents number of recorded MSNs.

Table 1.

Active and passive electrical properties of NAcSh MSNs.

Parameter	shControl MSN	shFABP MSN
RMP (mV)	−79.73±1.763 (n=19)	−66.06±4.176 ** (n=20)
Vthr (mV)	−39.13±1.948 (n=19)	−36.94±1.609 (n=20)
Ithr (pA)	49.47±7.029 (n=19)	58.5±7.081 (n=20)
Rin (MΩ)	239.3±14.78 (n=17)	224.4±18.42 (n=14)
Tau (msec)	16.64±1.62 (n=17)	18.93±1.679 (n=14)
Cm (pA/pF)	69.82±4.94 (n=17)	87.17±6.435 * (n=14)

RMP –resting membrane potential, Vthr – voltage threshold, Ithr – current threshold, Rin – input resistance, Tau – time constant, Cm – membrane capacitance. All values are mean ± standard error.

** $p<0.01$;

* $p<0.05$ with Student's *t*-test.